

## CFD ANALYSIS OF A DENSITY-DEPENDENT VALVE WITHIN A HOT WATER SYSTEM

Helen Smith, Sally S. Bell, John N. Macbeth, David C. Christie, Neil Finlayson

Greenspace Research, Lews Castle College UHI, Stornoway, Isle of Lewis, United Kingdom  
HS2 0XR

**Key words:** Fluid Dynamics, Renewable Energy, Valve

**Abstract.** *The design of a buoyancy valve for a renewable energy thermal storage tank led us to this interesting CFD problem. The purpose of the valve is to allow water to circulate within the system when the temperature of the water rises above a critical value. From Archimedes principle, a buoyancy float made from a given material will rise (providing a closed state for the valve) when below a critical temperature and sink (providing an open state for the valve) when above a critical temperature. However, the precise valve response depends on internal temperature and mass-flow dynamics. In this paper, we present a CFD investigation of the valve's behaviour under specific conditions.*

## 1 Introduction

The Outer Hebrides of Scotland offers some of the richest wind resources in the world, coupled with substantial amounts of solar energy in the summer months. Our overall aim is to design and test a thermal storage system for use in a Hebridean context that promotes high system efficiency when charged by an intermittent renewable energy-driven electrical supply. This will offer an efficient solution to the heating and provision of domestic hot water within buildings, and offers the potential for scaling to district heating schemes. The energy resource exhibits a high degree of intermittency, with hourly, daily and seasonal variances. This must be addressed with effective control mechanisms involving flow regulators and inlet/outlet diffusers to modulate the flow-rate and maximise stratification [8, 10, 2, 9, 5].

The degree of stratification is an important determinant of efficiency for a thermal storage unit. In a well stratified tank, hot layers of fluid accumulate above the cooler layer, with minimal mixing. This increases the useful energy content of the system. For example, stratification enables many solar water heating systems to cope with the diurnal patterns of energy from the sun, along with energy fluctuations over a shorter timescale[10, 7, 6]. During charge cycles, the hot water returning from the solar collector is, in some designs, introduced to the area of the tank that is closest in temperature. During the discharge cycle, mixing is avoided by introducing the cold water at the bottom of the tank, and taking the hot water out at the top. Mechanisms to promote stratification involve combinations of temperature sensors, inlet or outlet diffusers and valves which add and remove water from areas of the tank according to desired temperature and flow-rate control functions.

The thermal storage system envisaged by the authors is intended to deliver water at a constant temperature under conditions of intermittent energy supply, which could be from a system of wind turbines, or possibly even a biomass stove. As shown in Figure 1, the cold water is removed from the tank, heated in a side-arm and returned to the top of the tank at a temperature as close to the set point as possible. To make the system as passive as possible the fluid circulation is achieved using a thermosyphon. The transient nature of such a setup[3] poses interesting dynamics problems which the authors hope to investigate further in the future.

The power delivered to the heater is assumed to be independent of temperature but of variable magnitude. Thus, the correct mass flow rate through the side arm must be achieved in order to obtain the desired set point temperature. This mass flow rate is given by

$$\dot{m} = \frac{\dot{Q}}{c_p \Delta T}. \quad (1)$$

In the absence of such mass flow throttling, the fluid would accelerate until the driving force equalled that of the friction losses in the pipes. A runaway flow rate would cause the fluid to leave the heating arm at a reduced temperature, and destroy the stratification.

□

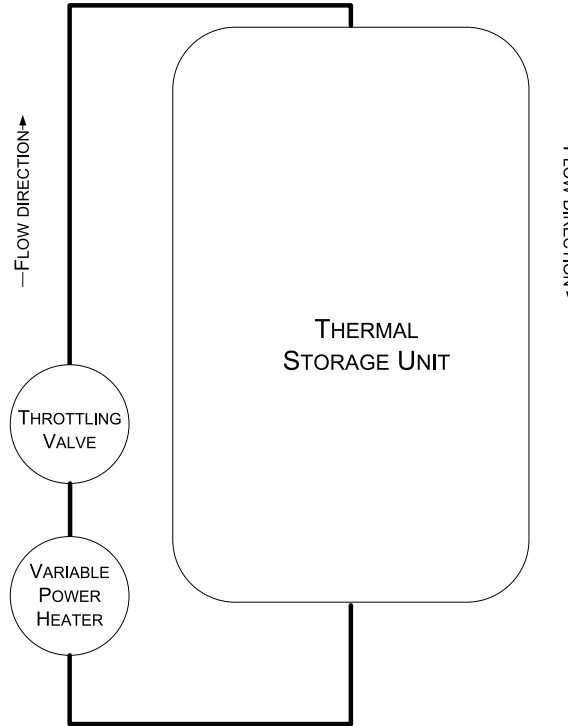


Figure 1: Schematic of overall tank design.

To control the mass flow rate, a throttling valve is required. Due to the low driving forces and in turn the low pressure drops, commercially available thermostatic valves are often found to be inadequate for this purpose. The need for a large opening area combined with small driving forces makes a large thermostatic valve the only available choice, but these tend to suffer from chattering under these conditions due to the very low flow rates.

We are exploring the possibility of controlling the fluid flow using a density-dependent buoyancy valve that only allows water to circulate within the system when the temperature of the water rises above a critical value. The key role of the valve in regulating the dynamical behaviour of the whole system means that its behaviour and response to varying temperature must be well understood. Hence, we are using CFD to build up as comprehensive a picture of its properties as possible.

## 2 Modelling the Buoyancy Valve

The buoyancy valve is an important element in the thermal storage system, as it provides the controller functionality for the system. An ideal valve has a simple off-on switching with an instantaneous transition from zero to on-state mass flow rate. In reality the valve will have a finite off-on rise-time and may exhibit ringing and instability.

A float made from a given material will rise (providing a closed state for the valve) when below a critical temperature and sink (providing an open state for the valve) when above a critical temperature, as shown in Figure 2.

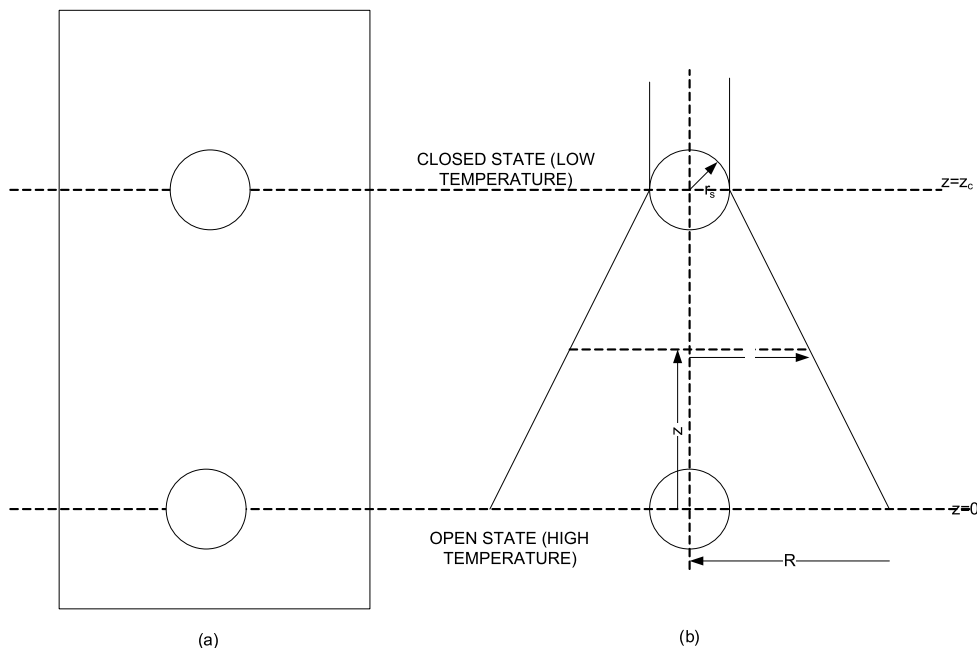


Figure 2: (a) Buoyancy float in beaker (b) Schematic of buoyancy valve

If the only forces acting on the float were due to buoyancy, the equation of motion would simply be

$$\frac{d^2z}{dt^2} = \frac{g}{\rho_s} (\rho_w - \rho_s) \quad (2)$$

where  $z$  is the height of the float,  $g$  is the gravitational acceleration,  $\rho_s$  is the density of the float, and  $\rho_w$  is the density of the water.

If the temperatures and hence the densities were fixed, Equation (2) can be trivially integrated to give

$$z = \frac{g}{2\rho_s} (\rho_w - \rho_s) t^2 + v_0 t + z_0 \quad (3)$$

where  $v_0$  and  $z_0$  are the initial vertical speed and position. The time taken for the float to rise or sink a distance  $h$  from a standing start would then be

$$t = \left( \frac{2\rho_s h}{g(\rho_w - \rho_s)} \right)^{\frac{1}{2}}. \quad (4)$$

However in the real system, the temperature is not fixed, and changes dynamically. Heat transfer through the fluid volume takes place gradually, and heat transfer rates

between the sphere and the water must be taken into account. Convection can take place, and convective acceleration within the valve is also a factor. As a result of all these factors, the mass flow rate through the valve is choked off gradually rather than instantaneously.

A CFD approach to modelling the system is useful to investigate these dynamics. Here we analyse the effect of heating on a spherical float submerged within a beaker of water. For simplicity, we assume that the float has a constant density, and we linearise the density of the water around the critical temperature,  $T_C$ . The densities chosen are

$$\rho_s = 987.635 \text{ kg m}^{-3}, \quad \rho_w = -0.4527T_w + 1134.3 \text{ kg m}^{-3} \quad (5)$$

$T_C$ , the theoretical critical temperature at which the densities are equal, is 323.978K.

A 3-D model of the experiment was produced in Solidworks and then imported into a commercially available CFD programme, CD-adapco's Star-CCM+. The mesh was generated within Star-CCM+ using a base size of 0.01m for the surface and volume mesh (trimmer mesh). A volumetric control (cuboid) was introduced over the water surface to allow a tighter mesh at the air/water interface. To form the tighter mesh, the base size of the surface mesh and the volume mesh ( $z$ -direction only) within the volumetric control were reduced to 0.002m.

The base and sides of the beaker were defined as no-slip walls and the top of the beaker was defined as a pressure outlet. The sphere is actually a hole in the mesh with the surrounding mesh defined as a wall. This also had a tighter mesh with the target base size specified as 0.005m and the minimum base size specified as 0.0015m.

The simulations considered a three-dimensional model for the simulation with no symmetry planes and solved using a First-Order temporal scheme (Euler Implicit). The time-step was set as 0.01 seconds with the stopping criteria for maximum inner iterations defined as 5. The water and air in the beaker were defined as only one region but a mixture of two different Eulerian phases. A multiphase segregated flow model (SIMPLE algorithm) was used to solve a set of conservation equations for each Eulerian phase (air and water)[1, 11]. Thermal effects were also included in the segregated model. The flow was assumed to be laminar and gravity was considered. The sphere was defined as a 6-DOF body, given a mass of 0.0246943kg and released from its starting position at 0.01s. The float was constrained to move only in the vertical ( $z$ -direction) and was not allowed to rotate. The density of the sphere is defined to be constant and the density of the water changes linearly with temperature (see Equation (5)).

### 3 Water at constant temperature

The first situation to be modelled was the float, initially at rest, immersed in water at a constant temperature. This allowed comparison to be made between the numerical CFD results and the simple theoretical predictions. It also enabled the critical temperature to be verified in the simulation.

The temperature is invariant both temporally and spatially. One would expect that,

apart from the effects of drag, the displacement of the float would not deviate much from the behaviour predicted by Equation (3). The trajectories of the float, calculated with the CFD code, are plotted in Figure 3 for various water temperatures. As expected, the curves appear parabolic, and the float is observed to sink when the water temperature exceeds a critical temperature, and to rise when the water is colder than this  $T_C$ . For comparison, the set of curves in Figure (4) gives the trajectories predicted by Equation (3). The major difference between the sets of plots is the value of the critical temperature. In the simulated curves, the float rises in water at 326.9K and sinks and 327.9K, putting the critical temperature somewhere between these two values. The theoretical results show the sphere floating at 324.1K and sinking at 323.1K, consistent with the theoretical critical temperature being 323.978K.

Further simulations were carried out in order to close in on the CFD code’s value of the critical temperature. A value of 327.8K was obtained, 3.7K above the value predicted by comparing the densities.

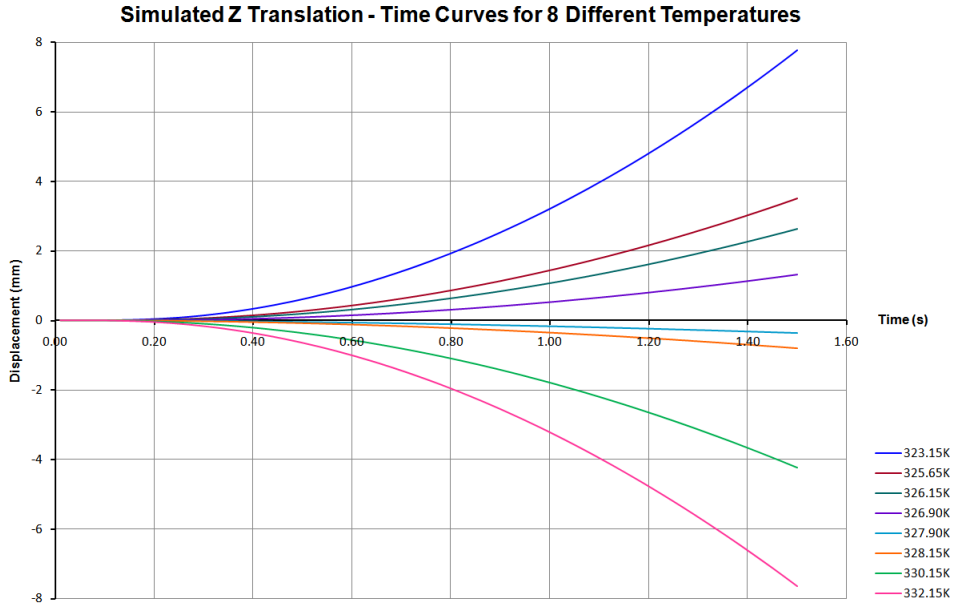


Figure 3: Trajectories of the float immersed in water of various temperatures, according to the CFD code. The CFD code was run using a commercially available CFD programme (CD-adapco Star-CCM+).

The time taken in the CFD simulation for the float to travel 0.3mm through water of various temperatures is plotted in Figure 5. Figure 6 shows a plot of the sink and rise times predicted by Equation (4). The results are qualitatively similar, with the sink and rise times tending to infinity as the critical temperature is approached. Again, the chief difference is the value of the critical temperature. This could potentially be a result of the mesh used, and it is hoped that, with additional computational time, this discrepancy can be investigated further.

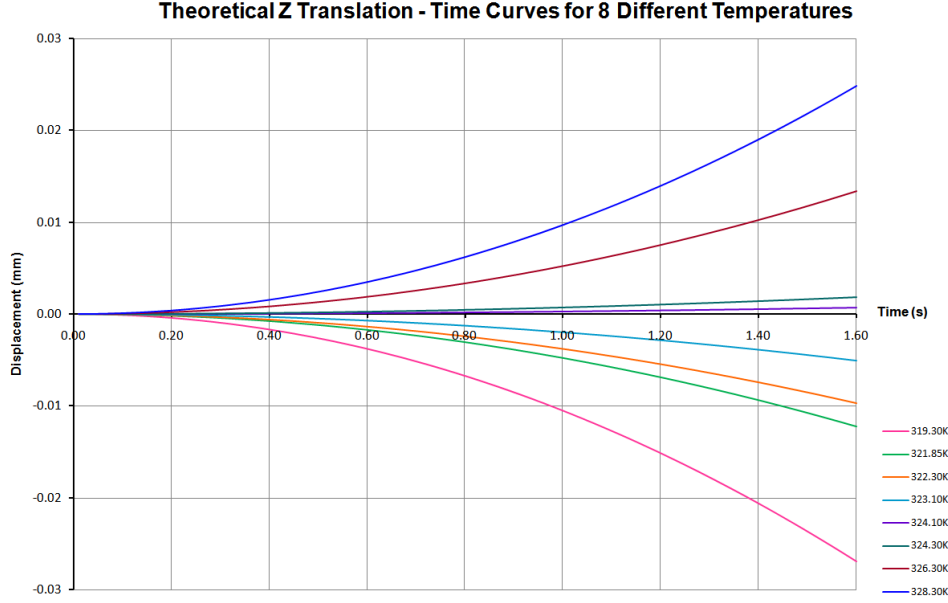


Figure 4: Trajectories of the float immersed in water of various temperatures predicted by Equation (3).

#### 4 Water heated from below

Having established a critical temperature, the next step is to investigate the motion of the float as the water is heated through this point. The speed of response is one of the factors that will determine the float's suitability as a valve.

A heat flux of  $\Phi_q$  is supplied to the base of the beaker, which contains the float, as well as a volume  $V$  of water. An initial, qualitative estimate of the float's motion can be obtained by assuming that temperature of the water is spatially uniform. This temperature is then given by

$$T_w = T_i + \frac{\Phi_q A}{cm} t \quad (6)$$

where  $A$  is the area of the beaker's base, and  $m$  is the mass of the water, and  $c$  is its specific heat capacity (which we evaluate at the set-point temperature). If the density of the float is  $\rho_s$  and the density of the water is  $\rho_w = \rho_0 + \alpha_w T_w$ , the equation of motion (2) can be integrated to give

$$z = \frac{g\Phi_q A \alpha_w}{6cm\rho_s} t^3 + \frac{g}{2\rho_s} (\rho_0 - \rho_f + \alpha_w T_i) t^2 + v_0 t + h_0 \quad (7)$$

where  $v_0$  and  $h_0$  are the initial vertical speed and position. As before,  $\rho_s = 987.635 \text{ kg m}^{-3}$ ,  $\alpha_w = -0.4527$ , and  $\rho_0 = 1134.3 \text{ kg m}^{-3}$ . The mass of water is 3.95kg, and its specific heat capacity is taken to be  $4183 \text{ J kg}^{-1} \text{ K}^{-1}$ . We consider a heat flux of  $100 \text{ kW m}^{-2}$ , which corresponds to a total heating power of 2kW. The float trajectories were calculated

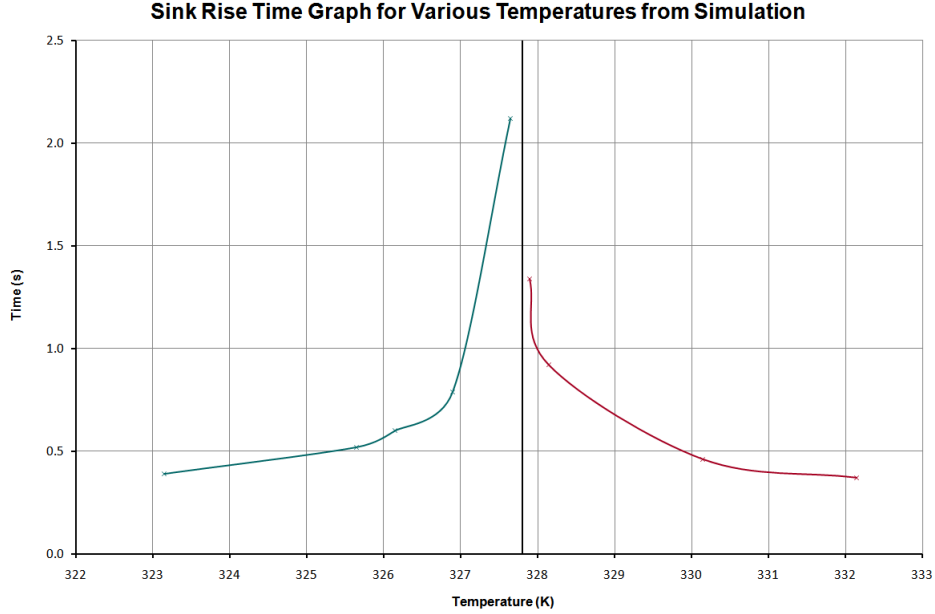


Figure 5: Sink and rise times from the simulation. The blue line on the left indicates rise times, while the red line on the right indicates sink times.

for starting temperatures of 0.275K below the critical temperature (323.703K) and 0.4K below  $T_C$  (323.578K), and are plotted in Figure 7.

Equation (7), and the resulting plots in Figure 7 give a qualitative idea of the behaviour of the float, but rely on the assumption that the water is being heated uniformly. This is likely to lead to an underestimation of the time taken for the float to react, as it assumes that the heat flux from the bottom is transmitted instantaneously to the region containing the float.

A more comprehensive analysis of the temperature distribution in the fluid would involve solving the temperature diffusion equation[4]:

$$\frac{\partial T}{\partial t} + (\mathbf{v} \cdot \nabla) T = \lambda \nabla^2 T \quad (8)$$

(where  $\lambda = \frac{k}{\rho c_p}$  is the thermal diffusivity), coupled with the Navier-Stokes equation for the fluid velocity field  $\mathbf{v}$ :

$$\frac{\partial \mathbf{v}}{\partial t} + (\mathbf{v} \cdot \nabla) \mathbf{v} = -\frac{\nabla P}{\rho} + \mathbf{g} + \nu \nabla^2 \mathbf{v} \quad (9)$$

where  $\nu$  is the kinematic viscosity and  $P$  is the pressure. This pair of equations can be solved subject to the no-slip boundary conditions for the velocity field and appropriate boundary and initial conditions for the temperature. For an insulated container with a specified heat flux at the base, a suitable boundary condition would be the Neumann

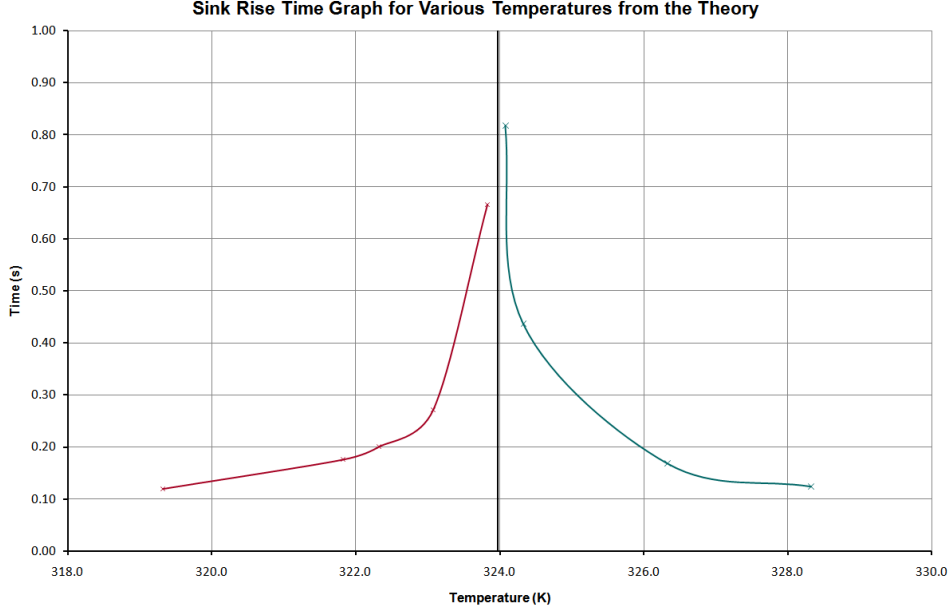


Figure 6: Sink and rise times predicted by Equation (4). The blue line on the left indicates rise times, while the red line on the right indicates sink times.

condition

$$-k\partial_z T = \begin{cases} \Phi_q & \text{at } z = 0, \\ 0 & \text{on the other bounding surfaces.} \end{cases} \quad (10)$$

In general, such a system will be difficult to solve. However, the problem may be simplified by setting the velocity field to zero (pure conduction) and assuming that the solutions are independent of  $x$  and  $y$ . The diffusion equation (8) and boundary condition (10) would then simplify to

$$\frac{\partial T}{\partial t} = \lambda \frac{\partial^2 T}{\partial z^2} \quad (11)$$

with

$$-k\partial_z T = \begin{cases} \Phi_q & \text{at } z = 0, \\ 0 & \text{at } z = h \end{cases} \quad (12)$$

where  $h$  is the height of the container. A simple solution would be

$$T = -\frac{\Phi_q \lambda}{hk} t - \frac{\Phi_q}{2hk} z^2 + \frac{\Phi_q}{k} z + T_0. \quad (13)$$

This does not satisfy an appropriate initial condition of a uniform temperature at  $t = 0$ , but may in some sense be considered an asymptotic solution after some time has elapsed. This solution must however be considered unsatisfactory as it expressly rules out the convection effects one would expect to see in a container of water heated from below

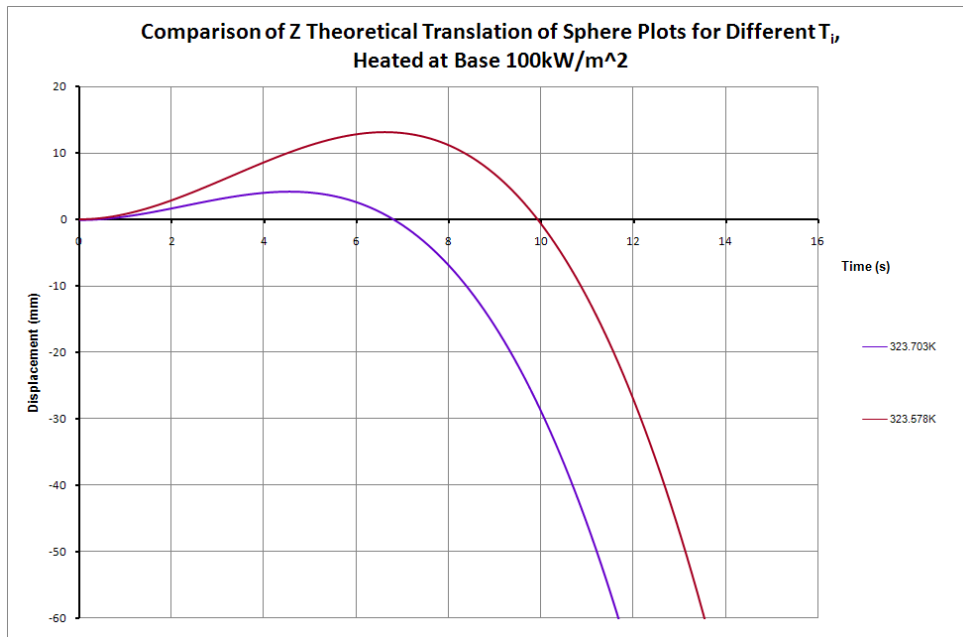


Figure 7: Trajectories of float in water with 2kW of heating, with various starting temperatures, calculated using the uniform-heating approximation given by Equation (7).

(and its stability with respect to small perturbations in the velocity field is unclear). The solution (13) could thus be considered as overly simplistic. Yet, when inserted into the equation of motion (2) for the float, the temperature (13) yields to a non-linear partial differential equation that does not appear to be amenable to analytic solution.

Thus, we must turn to CFD simulation for further insight into the problem. We used the same model and conditions as described earlier for the constant water temperature but allowed the base to be heated. We heat the base with a heat flux of  $100 \text{ kW m}^{-2}$ , and set an initial condition of constant water temperature for the volume of water within the beaker. The vertical displacement of the sphere was investigated for a range of initial temperatures below the critical temperature. Figure 8 shows the vertical displacement of the sphere at a selection of initial temperatures comparable to those seen in the earlier theoretical findings (Figure 7). The theoretical results, Figure 7, consider starting temperatures of  $T_C - 0.275K$  and  $T_C - 0.4K$ . However, to take account of the different critical temperatures, the initial temperatures considered for the CFD results, Figure 8, are  $0.275K$  and  $0.4K$  below the critical temperature found in earlier simulations ( $323.703K$ ).

The CFD and theoretical findings are qualitatively similar, exhibiting the same behaviour of initially rising and then falling (when temperature of water is heated through critical temperature). The theoretical results assume that the water is heated uniformly, so as expected the sphere takes longer to respond to heating when examined with the CFD. This is because the water is not heated uniformly and also because as the sphere rises, it is rising into cooler regions (this can be seen more clearly in Figure 9).

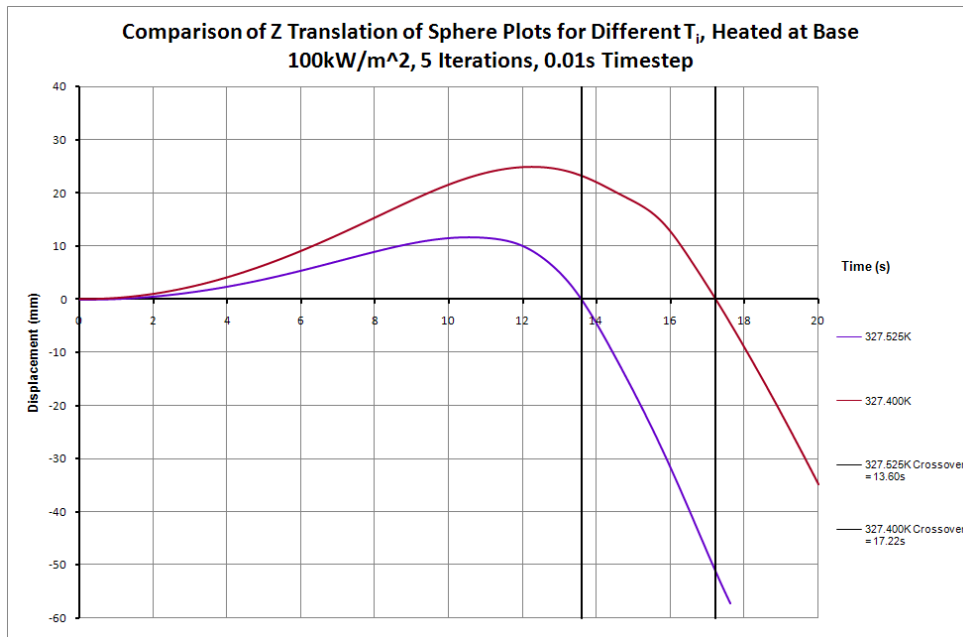


Figure 8: Simulation heated - can be updated tomorrow or later today. The CFD code was run using a commercially available CFD programme (CD-adapco Star-CCM+).

## 5 Discussion

The use of CFD analysis in the design of this buoyancy driven density-dependent valve has allowed us to gain greater insight into the problem than would have been possible from theoretical results alone. Our simulation results from CFD displayed the same qualitative behaviour as we expected given the theoretical results. The sphere rose when below a critical temperature (valve closed) and sank when above it (valve open). We also observed a transition from an initial starting point to a closed state and then an open state when the water was heated through the critical temperature. However, the critical temperature observed in the CFD simulations differed from the theoretical value. One explanation for this discrepancy could be the coarseness of the mesh on the sphere boundary and we hope to refine the mesh in the future.

The sphere took longer to respond to heating in the simulation than expected from the theory. This is because the theory assumed the water would heat uniformly and did not allow for the effects of convection. It was this requirement for assumptions within the theoretical problem which led us to use CFD for further investigation of the problem. We believe the CFD greatly improved our understanding of the transient dynamics of the system as a whole.

The research will be further extended by including a material in the sphere, rather than a hole in the mesh, and studying the time-delays caused by the thermal conductivity of the material. This would allow us to consider a range of different materials and assess their suitability for this application. Our CFD model currently restricts the sphere to

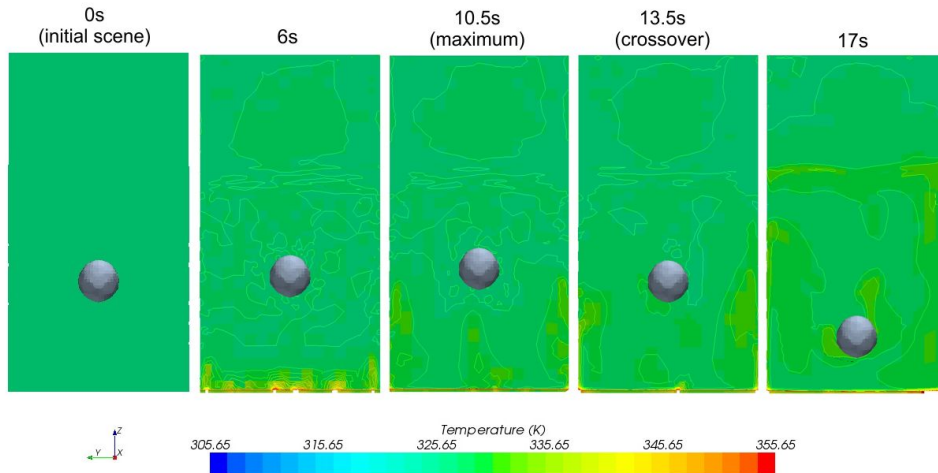


Figure 9: Temperature of fluid in beaker through time in one simulation. The initial temperature of the water is 327.525K with a heat flux of  $100 \text{ kW m}^{-2}$  applied to the base. The CFD code was run using a commercially available CFD programme (CD-adapco Star-CCM+).

vertical movement only (translation in  $z$ -direction). This will be extended to consider both translation and rotation in  $x$ ,  $y$  and  $z$  directions. Following these extensions, we hope to conduct laboratory experiments to validate our CFD results.

In order to allow this work to further aid in the valve design process, we hope to use CFD to examine a set-up similar to the schematic seen in Figure 2. This would involve including a flow through a pipe and should give us greater insight into the valve's suitability for the physical application. This can then be further refined to examine the valve capabilities within the tank design as whole.

## REFERENCES

- [1] J D Anderson JR. *Computational Fluid Dynamics, The Basics with Applications*. McGraw-Hill, Inc., USA, 1995.
- [2] A Aviv, Y Blyakhman, O Beeri, G Ziskind, and R Letan. Experimental and numerical study of mixing in a hot-water storage tank. *Journal of Solar Energy Engineering*, 131:011011, 2009.
- [3] Kyle S Benne. *Transient performance of closed loop thermosyphons incorporating thermal storage*. PhD thesis, University of Missouri-Rolla, 2007.
- [4] J K Bhattacharjee. *Convection and Chaos in Fluids*. World Scientific, Singapore, 1987.
- [5] C. Cristofari, G. Notton, P. Poggi, and A. Louche. Influence of the flow rate and the tank stratification degree on the performances of a solar flat-plate collector. *International Journal of Thermal Sciences*, 42(5):455 – 469, 2003.
- [6] Simon Furbo, Elsa Andersen, Sren Knudsen, Niels Kristian Vejen, and Louise Jivan Shah. Smart solar tanks for small solar domestic hot water systems. *Solar Energy*, 78(2):269 – 279, 2005. ISES Solar World Congress 2003.
- [7] Y M Han, R Z Wang, and Y J Dai. Thermal stratification within the water tank. *Renewable and Sustainable Energy Reviews*, 13(5):1014–1026, 2009.
- [8] K.G.T. Hollands and M.F. Lightstone. A review of low-flow, stratified-tank solar water heating systems. *Solar Energy*, 43(2):97 – 105, 1989.
- [9] S Knudsen and S Furbo. Thermal stratification in vertical mantle heat-exchangers with application to solar domestic hot-water systems. *Applied Energy*, 78:257–272, 2004.
- [10] Louise Jivan Shah, Elsa Andersen, and Simon Furbo. Theoretical and experimental investigations of inlet stratifiers for solar storage tanks. *Applied Thermal Engineering*, 25:2086–2099, 2005.
- [11] J Tu, G H Yeoh, and C Liu. *Computational Fluid Dynamics, A Practical Approach*. Butterworth-Heinemann, Oxford, UK, 2008.